Dyes and Pigments 184 (2021) 108773

Contents lists available at ScienceDirect

Dyes and Pigments

journal homepage: http://www.elsevier.com/locate/dyepig

Photoprocesses in bis(18-crown-6)-1,3-distyrylbenzene and its complexes with metal perchlorates

Levon S. Atabekyan [a], Alexandra Ya Freidzon [a,c,*], Alexander K. Chibisov [a], Sergey P. Gromov [a,b], Sergey Z. Vatsadze [b], Vyacheslav N. Nuriev [b], Alexey V. Medvedko [b]

[a] Photochemistry Center of RAS, FSRC Crystallography and Photonics, Russian Academy of Sciences, Novatorov Str. 7A-1, Moscow, 119421, Russian Federation
[b] Department of Chemistry, M.V. Lomonosov Moscow State University, Leninskie Gory 1-3, Moscow, 119991, Russian Federation
[c] National Research Nuclear University MEPhI (Moscow Engineering Physics Institute), Kashirskoye Shosse 31, Moscow, 115409, Russian Federation

ARTICLE INFO

Keywords:
1,3-distyrylbenzene
Fluorescence
Complexation
Laser flash photolysis
Triplet state
Quantum chemical calculations
DFT and TDDFT calculations
Excited states

ABSTRACT

Photoprocesses of bis(18-crown-6)-1,3-distyrylbenzene (DSB) and its complexes with barium and lead perchlorates in a MeCN–CH_2Cl_2 (9:1, v/v) mixture were studied by absorption, luminescence, and laser kinetic spectroscopies. Unlike its strongly conjugated 1,4-isomer, 1,3-derivative shows almost independent behavior of its chromophoric subunits and is capable of phototransformations not observed in 1,4-distyrylbenzenes. Triplet DSB complexes are involved in the radiationless deactivation of the excited state along with the fluorescence processes. The most effective intersystem crossing was observed for the complex with lead perchlorate. The process is accompanied by a drastic decrease in the quantum yield of DSB fluorescence. Quantum chemistry (DFT and TDDFT) is used to calculate the geometric structure and absorption spectra of DSB and its complexes with barium and lead cations and to explain the observed results.

1. Introduction

The interest to the crown-containing unsaturated compounds arises from their ability to self-assembly into supermolecules and supramolecular ensembles through complexation with metal or ammonium cations. As a result, their spectral characteristics change noticeably. In addition, they can change their structure and properties upon irradiation [1]. Typical photochemical processes that take place in these crown-containing supramolecular systems and involve substantial changes in their properties are *trans-cis* photoisomerization and [2 + 2]-photocycloaddition [2–4].

The presence of two C=C double bonds in the structure of distyrylbenzenes ensures additional possibilities for molecular photoswitching [5,6] and relatively high fluorescence quantum yields [7,8]. These and other interesting properties make distyrylbenzenes promising for the design of photoactive materials, such as emitters for organic light emitting diodes, absorbers for solar cells, active media for nonlinear optics, chemical sensors, etc. [9–14]. Distyrylbenzenes fall into three groups depending on the substitution type in the central benzene ring. 1, 2-Disubstituted ones fall beyond the scope of our research [15]. The spectral and photophysical properties of bis(18-crown-6)-1, 4-distyrylbenzene (***1*** in Scheme 1) and its complexes with metal cations were investigated previously [16,17]. 1,3-Distyrylbenzenes are poorly studied. Only few functional derivatives of them are known, all containing substituents in the terminal and central benzene moieties [18,19]. They exist as a mixture of several rotamers that can be distinguished by their photochemical and photophysical properties. In particular, their fluorescence decay is not always monoexponential [20]. The chemical and photochemical properties of 1,3-distyrylbenzenes differ from those of their strongly conjugated 1,4-isomers owing to less conjugation between the styryl moieties [20–23].

Biscrown-containing 1,3-distyrylbenzenes were synthesized only recently [24]. In them, one may expect as diverse photochemical behavior and pronounced complexing capacity as in biscrown-containing stilbenes [25,26] and 1,4-distyrylbenzenes [16]. However, high potential of biscrown-containing 1,3-distyrylbenzenes as building units for complex photoactive supramolecular ensembles is yet to be understood. Therefore, the goal of this paper is to study

* Corresponding author. Photochemistry Center of RAS, FSRC "Crystallography and Photonics", Russian Academy of Sciences, Novatorov str. 7A-1, Moscow, 119421, Russian Federation.
E-mail addresses: levat51@mail.ru (L.S. Atabekyan), freidzon.sanya@gmail.com (A.Y. Freidzon), alexander.chibisov@gmail.com (A.K. Chibisov), spgromov@mail.ru (S.P. Gromov), szv@org.chem.msu.ru (S.Z. Vatsadze), nvn@org.chem.msu.ru (V.N. Nuriev), lexeym@gmail.com (A.V. Medvedko).

https://doi.org/10.1016/j.dyepig.2020.108773
Received 14 May 2020; Received in revised form 7 July 2020; Accepted 8 August 2020
Available online 18 August 2020

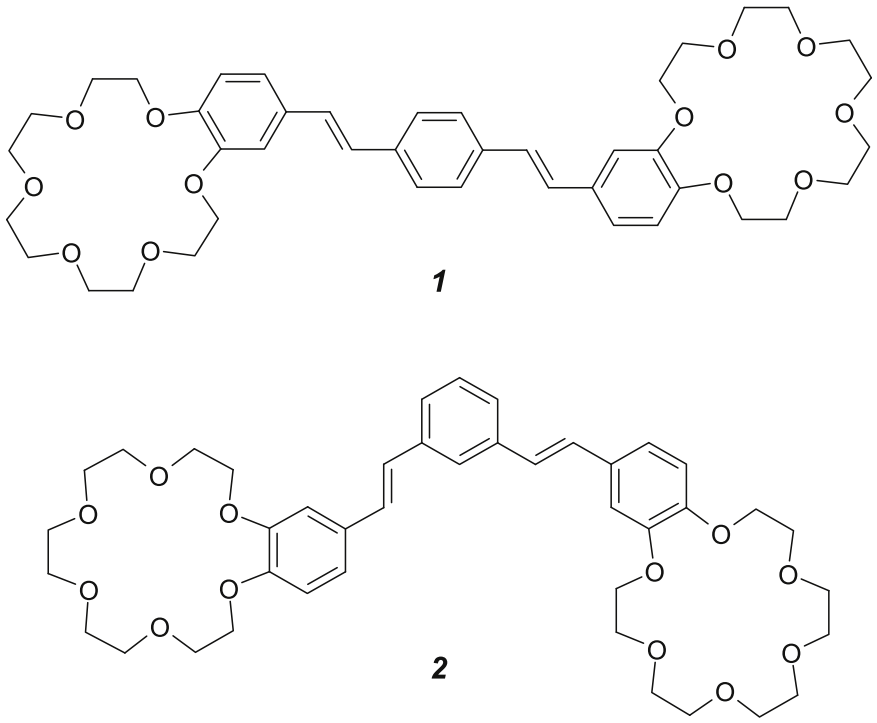

Scheme 1. Structurs of ***1*** and ***2***.

photoprocesses of bis(18-crown-6)-1,3-distyrylbenzene (***2*** in Scheme 1) and its complexes with metal cations, as potential photoswitches or photosensors, to detect the intermediates of photoreactions (in particular, the triplet state of ***2*** and its complexes), and to compare the properties of compounds ***1*** and ***2***.

We used barium and lead perchlorates for complexation. These cations were chosen because of their high complexation constants observed with other 18-crown-6-containing ligands [16,27,28]. In addition, lead was chosen, because it is a typical heavy atom, which induces intersystem crossing of the dye to the triplet state upon complexation [29].

Our experimental studies were supported by DFT quantum chemical calculations to elucidate the changes in the chromophore structure and to explain the experimentally observed spectral shifts upon complexation.

2. Experimental

Bis(18-crown-6)-1,3-distyrylbenzene ***2*** was synthesized according to the procedure described in Ref. [24]. The synthesis protocol and characterization data (^{1}H NMR, ^{13}C NMR, mass spectrum and elemental analysis) are given therein.

The ground-state absorption spectra of ***2*** were recorded on an Agilent 8453 spectrophotometer (Agilent, USA). The luminescence spectra were recorded on a Varian Eclipse spectrofluorimeter (Agilent, USA). The difference absorption spectra of photoreaction products and the kinetics of their transformations were measured by means of a nanosecond pulsed laser photolysis setup [30] using a third harmonic of a Solar laser (Solar Laser Systems, $\lambda = 355$ nm, 20 ns pulse). Dissolved oxygen was removed by bubbling argon through the solution within 20–30 min. We believe that this is sufficient to completely remove oxygen from the solution. Steady-state irradiation of the dye solutions was performed using a DKSSh-150 lamp with an UFS-2 light filter. The fluorescence quantum yields were measured relative to 9,10-diphenylanthracene (quantum yield is 0.92 in ethanol [31]) to an accuracy of 10%. Lead perchlorate trihydrate and barium perchlorate (Merck) were used without purification. Measurements were carried out in a MeCN:CH_2Cl_2 (9:1, v/v) mixture using "extra pure 0" MeCN (Cryochrom NPK Ltd., Russia) and CH_2Cl_2 (Aldrich). All measurements were carried out at room temperature.

3. Computational details

The calculations were performed in order to explain the experimental absorption spectra and to determine the excited state energies of ***1*** and ***2*** and their complexes with Ba^{2+} and Pb^{2+} cations. The most stable rotamers of 1,3- and 1,4-distyrylbenzenes [16,24] were chosen for calculations. The geometry was optimized by DFT with PBE functional and 3z basis set [32] implemented in Priroda program package [33]. Stuttgart ECP46MWB pseudopotential [34] with corresponding basis set was used for Ba^{2+}; SBK pseudopotential [35] with corresponding basis set was used for Pb^{2+}. The absorption spectra were calculated by TDDFT with the PBE0 functional and SVP basis set [36] with solvent (MeCN) taken into account through D-PCM continuum solvation model [37]. In this case, the basis set for Ba^{2+} and Pb^{2+} used Stuttgart ECP46MWB and ECP60MWB pseudopotentials, respectively. These calculations were performed by the FireFly program package [38] partially based on GAMESS-US code [39]. The coordination spheres of Ba^{2+} and Pb^{2+} were saturated with four water molecules according to the computational procedure of Ref. [40]. It is known [41] that MeCN contains trace water (<0.005%, or ~10–3 mol/L, which is comparable to or higher than the metal concentrations used). Our previous calculations of alkali and alkaline-earth complexes with crown ethers [42–45] show that hard cations prefer coordination with hard ligands, such as water. As for lead, it also tends to prefer oxygen-containing ligands over nitrogen-containing ones. Therefore, we used only water to complete the coordination sphere of the cation. Ba^{2+} prefers asymmetrical coordination of water, while Pb^{2+} prefers symmetrical coordination. The triplet–triplet absorption spectra were calculated within Tamm–Dancoff approximation. The long-wave absorption spectra of the dyes and their complexes were built by Gaussian broadening of the vertical absorption lines with FWHM = 0.3 eV without taking into account the vibronic structure of the absorption band.

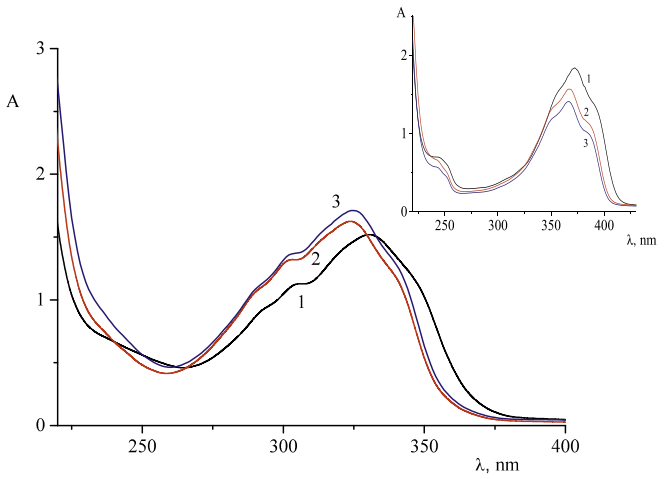

Fig. 1. Absorption spectra of ***2*** without (*1*) and with $Ba(ClO_4)_2$ (*2*) and $Pb(ClO_4)_2$ (*3*). The concentration of ***2*** is 2.5×10^{-5} mol/L; metal concentrations are 2×10^{-4} mol/L. Inset: Absorption spectra of ***1*** without (*1*) and with $Ba(ClO_4)_2$ (*2*) and $Pb(ClO_4)_2$ (*3*). The concentration of ***1*** is 2.5×10^{-5} mol/L; metal concentrations are 2.5×10^{-4} mol/L.

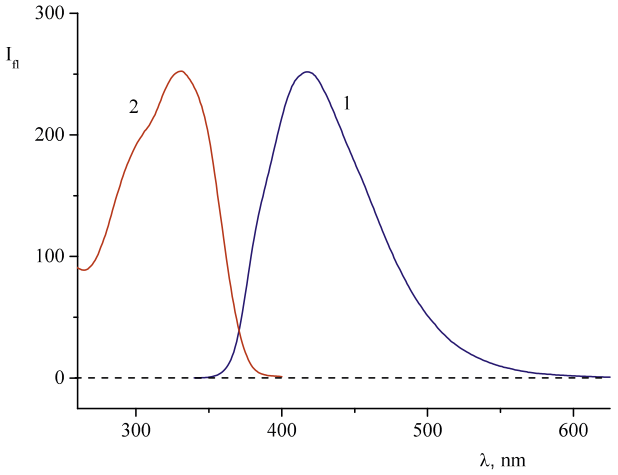

Fig. 2. Fluorescence emission (*1*) and excitation (*2*) spectra of ***2***. The concentration of ***2*** is 5×10^{-6} mol/L $\lambda_{exc} = 330$ nm (*1*), $\lambda_{fl} = 420$ nm (*2*).

4. Results and discussion

4.1. Electronic absorption and fluorescence spectra

Fig. 1 shows the absorption spectrum of ***2*** without (*1*) and with metal perchlorates (*2, 3*). The spectrum of ***2*** is poorly resolved and consists of a band at $\lambda_{max} = 330$ nm and two shoulders at 305 and 350 nm, which can be assigned to vibronic transitions.

1,3-Distyrylbenzenes absorb at shorter waves ($\lambda_{max} = 329–331$ nm) as compared to 1,4-distyrylbenzenes ($\lambda_{max} = 370–372$ nm), which originates from the efficient π conjugation in the entire chromophore in 1,4-derivatives. The conjugation in 1,3-disubstituted benzenes is much weaker; therefore, their absorption spectra can be considered as a sum of the spectra of two independent stilbene moieties. In all cases, the long-wave absorption bands are asymmetric and usually have a pronounced long-wave shoulder, which indicates the existence of several electronic transitions in their chromophore moieties with close energies due to multiple conformers [24].

In the presence of metal perchlorates, the absorption maximum in the spectrum of ***2*** is blue shifted by 5 nm, and the extinction coefficient increases, while the band shape remains the same. Similar shifts and band shape were observed in the spectrum of ***1*** [17]. Fig. 2 shows the fluorescence emission and excitation spectra of ***2***.

The fluorescence excitation spectrum of ***2*** virtually coincides with the absorption spectrum. A large Stokes shift (80 nm) is observed between the fluorescence emission and excitation maxima. The fluorescence spectra of ***2*** without (*1*) and in the presence of $Ba(ClO_4)_2$ (*2*) and

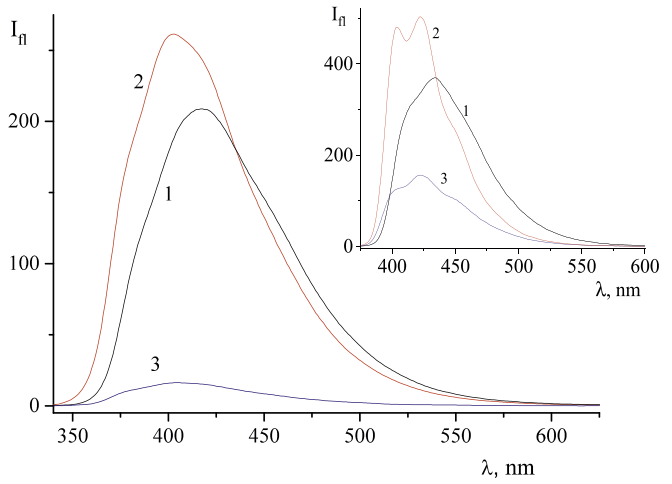

Fig. 3. Fluorescence spectra of ***2*** without (*1*) and with $Ba(ClO_4)_2$ (*2*) and $Pb(ClO_4)_2$ (*3*). The concentration of ***2*** is 5×10^{-6} mol/L; metal concentrations are 1×10^{-5} mol/L. Inset: Fluorescence spectra of ***1*** without (*1*) and with $Ba(ClO_4)_2$ (*2*) and $Pb(ClO_4)_2$ (*3*). The concentration of ***1*** is 2.5×10^{-6} mol/L; metal concentrations are 2.5×10^{-5} mol/L.

Table 1
Absorption band maximum (λ^{abs}_{max}), molar absorptivity ε_{max} at λ^{abs}_{max}, fluorescence band maximum λ^{fl}_{max}, and fluorescence quantum yield φ_{fl}.

Compound	*2*	*2* + Ba^{2+}	*2* + Pb^{2+}
ϕ_{fl}	0.41	0.46	0.03
λ^{fl}_{max}, nm	418	403	405
λ^{abs}_{max}, nm	331	324	325
ε_{max}, L/mol × cm^{-1}	6×10^4	7×10^4	7×10^4

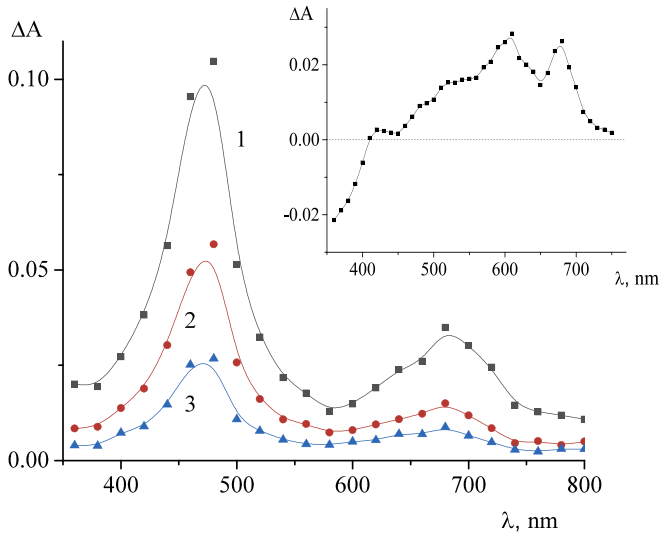

Fig. 4. Difference spectra of photoinduced absorption measured for oxygen-free solution of ***2*** at 1 (*1*), 50 (*2*) and 350 (*3*) μs after the laser pulse. The inset show the difference spectra of photoinduced absorption measured for oxygen-free solution of ***1*** at 5 μs after the laser pulse. The concentration of ***1*** is 5×10^{-5} mol/L, the concentration of ***2*** is 2.5×10^{-5} mol/L.

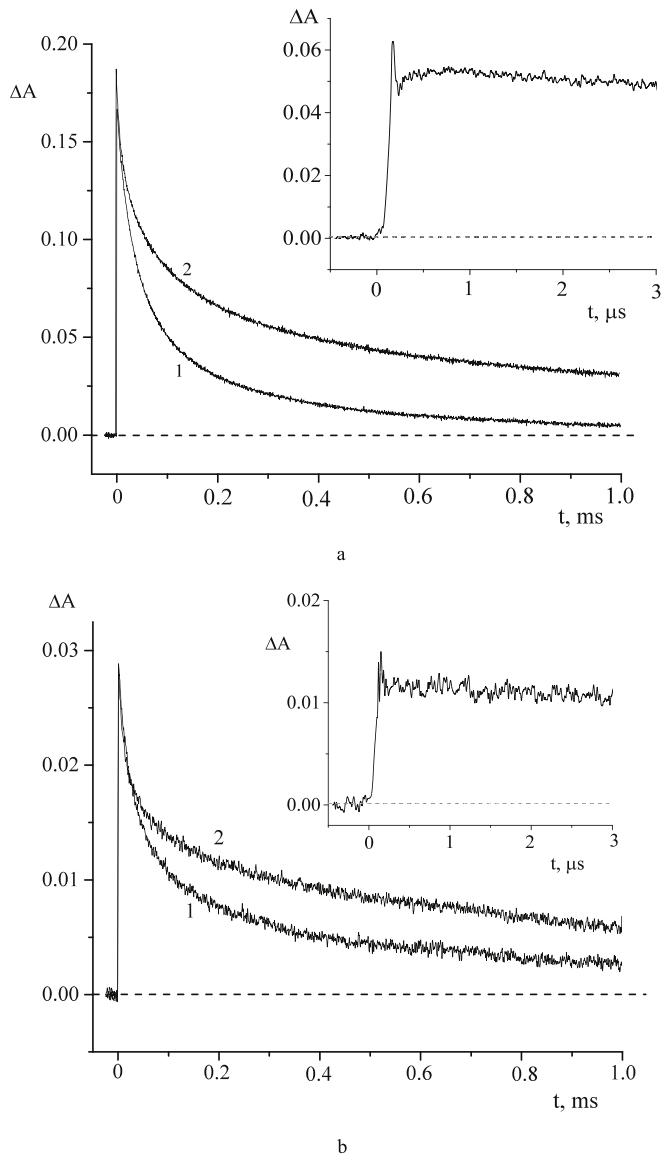

Fig. 5. Kinetic curves of the photoinduced absorbance change in the air-saturated (*1*) and oxygen-free (*2*) solution of ***2*** at λ = 480 nm (a) and 680 nm (b). Insets show the oscilloscope traces of the oxygen-free solution measured at an expanded time scale.

$Pb(ClO_4)_2$ (*3*) are shown in Fig. 3.

The fluorescence intensity slightly increases in the presence of barium cation, while with lead cation, the intensity decreases 14 times. The fluorescence band maxima are blue shifted by 15 nm. Table 1 gives the positions of the band maxima and fluorescence quantum yields of ***2*** and its complexes with lead and barium cations.

Note that the small difference in the absorption and fluorescence spectra of the free ***2*** and its complexes made determination of the complexation constants difficult.

4.2. Kinetic spectroscopy

Fig. 4 shows the difference spectra of photoinduced absorption measured upon laser irradiation of the oxygen-free solution of ***2***. The spectra were measured in 1, 50, and 350 μs after the laser pulse. The difference spectrum shows two pronounced photoinduced absorption bands at 400–550 and 600–750 nm.

Fig. 5 shows the kinetic curves of photoinduced absorbance measured in the band maxima of the difference spectrum at 480 and 680 nm. The insets show the kinetic curves of absorbance changes in the oxygen-free solution measured at an expanded time scale.

Table 2
Observed kinetics of the intermediates in the air-saturated and oxygen-free solutions of ***2*** measured at 480 and 700 nm.

λ, nm	Presence of oxygen	k_1, s^{-1}	k_2, s^{-1}
480	Air-saturated solution	2.8×10^4	4.2×10^3
	Oxygen-free solution	2.9×10^4	3.3×10^3
700	Air-saturated solution	3.0×10^4	3.4×10^3
	Oxygen-free solution	3.5×10^4	2.2×10^3

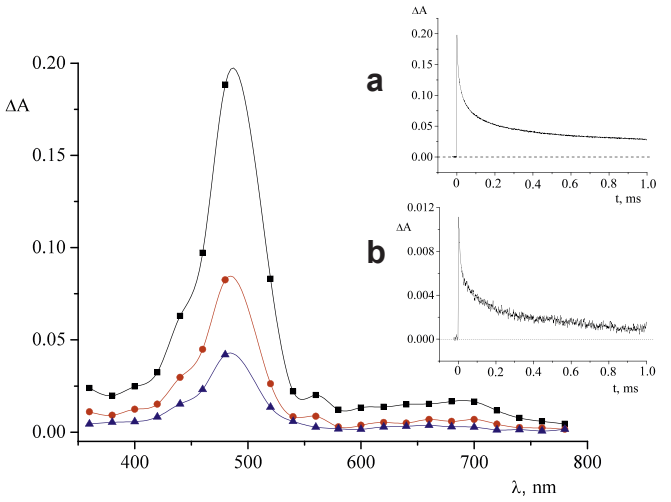

Fig. 6. Photoinduced absorption spectrum of oxygen-free solution of ***2*** in the presence of benzophenone measured at 1 (*1*), 50 (*2*) and 350 (*3*) μs after the laser pulse. The concentration of ***2*** is 2.5×10^{-5} mol/L; the concentration of benzophenone is 2.3×10^{-4} mol/L. The insets show the kinetic curves of the photoinduced absorbance at λ = 480 nm (a) and 700 nm (b).

The decrease in the lifetime of induced absorption in the presence of dissolved air oxygen can point to the triplet nature of the laser excitation intermediate. However, it is also possible that the product of laser irradiation can be free radicals formed as a result of a photochemical reaction.

In this case, the dissolved oxygen can react with radical species, which results in the decrease of the photoinduced absorption lifetime. The photoinduced absorbance kinetics is biexponential; Table 2 presents the observed rate constants measured at 480 and 680 nm. The measured kinetics of the photoinduced absorption in the microsecond timescale (insets of Fig. 5 (a,b)) made it possible to assign the short-lived intermediates at λ = 480 nm to those resulting from the two processes: a T-T absorption and an electron transfer. We can suppose that the latter process can take place as a result of the triplet-triplet dismutation [46]:

$$T + T \rightarrow R^{-}\bullet + R^{+}\bullet \quad (1)$$

From the energy point of view, such process is possible. Quantum chemical calculation shows that the energy of two relaxed molecules of ***2*** in the T1 state is ~0.5 eV higher than the sum energy of the radical cation and radical anion of ***2***. However, the detailed mechanism of the dismutation, if at all, is still to be elucidated.

The absence of quenching of the short-lived component by the air oxygen can indicate a short triplet lifetime. Therefore, in addition to the triplet state of ***2***, a relatively long-lived intermediate is formed after the laser pulse as well.

Fig. 5 (a,b) shows the kinetic curves typical of a long-lived intermediate, whose origin cannot be attributed to *E*–*Z*-isomerization. According to the quantum chemical calculation, (see below) that the absorption band of *Z*-isomer is blue shifted relative to the band of *E*-

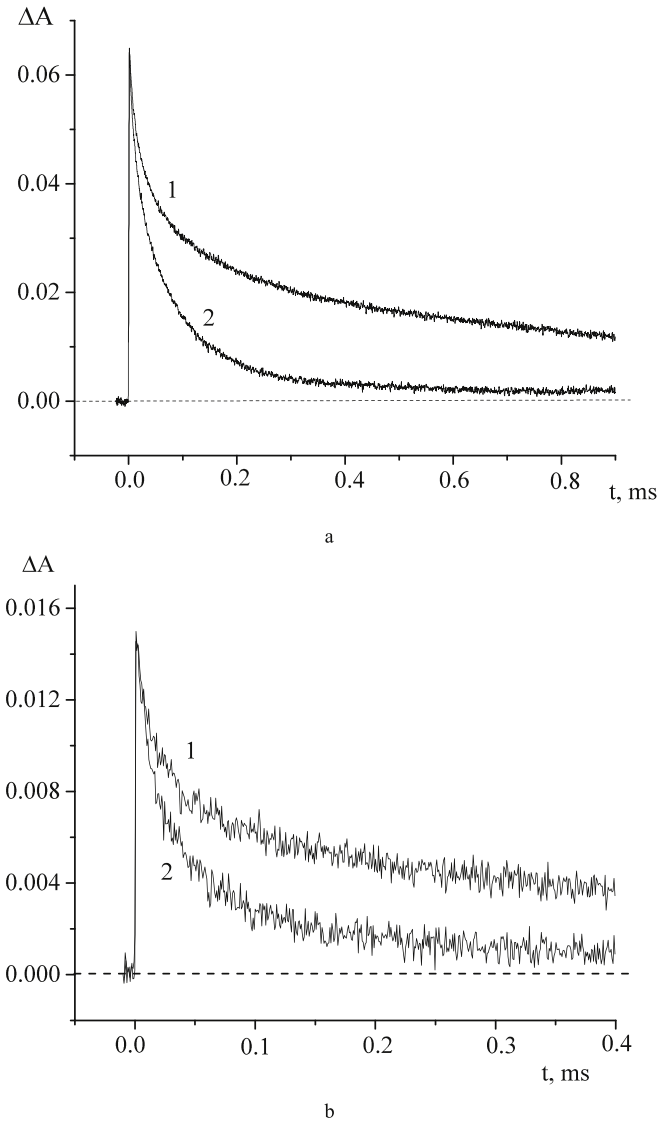

Fig. 7. Kinetic curves of the photoinduced absorbance of ***2*** without (1) and with (2) ascorbic acid: λ = 480 nm (a) and 680 nm (b). The concentration of ***2*** is 2.5×10^{-5} mol/L; the concentration of ascorbic acid is 2×10^{-4} mol/L.

isomer (λ_{max} = 330 nm, Fig. 1). This makes observation of *trans-cis* isomerization impossible under the current experimental conditions.

In order to support the idea that the triplet state is involved in the phototransformations of ***2***, the spectrum and kinetics of photoinduced absorbance changes in ***2*** were measured in the presence of benzophenone as a sensitizer. The experimental data are shown in Fig. 6.

The difference spectrum and kinetics of the photoinduced absorbance changes coincide with the similar data measured in the absence of benzophenone. However, benzophenone increases the yield of the photoinduced signal, which indicates an efficient triplet state population of the dye upon sensitized photoexcitation.

The T-T absorption of pure benzophenone is at 525 nm, and its triplet lifetime in a polar solvent is 50 μs [31]. This makes it possible to state that the difference spectrum and kinetic curves of Fig. 6 result from the sensitized population of the triplet state of dye ***2***.

Fig. 7 shows the kinetic curves of photoinduced absorbance measured at λ = 480 nm without (1) and with (2) ascorbic acid. The observed decrease in the lifetime of the reaction intermediate in the presence of the electron donor draws us to the conclusion that this intermediate can be associated with the radical cation of ***2*** ($R^{+}\cdot$).

No effect of both methyl viologen and *para*-nitroacetophenone as

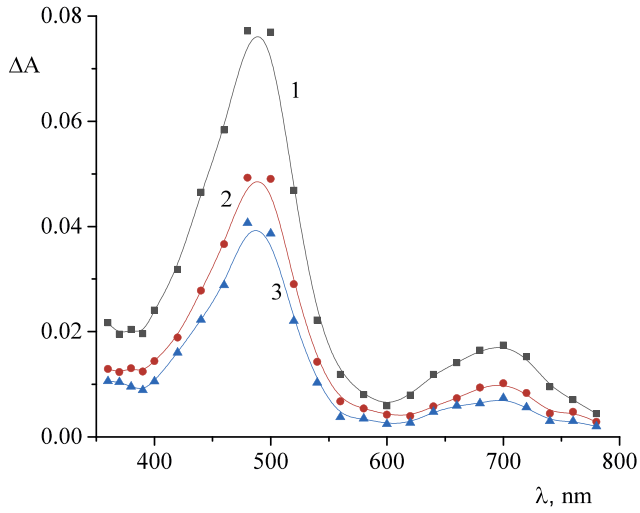

Fig. 8. Photoinduced absorption spectrum of the oxygen-free solution of ***2*** in the presence of $Ba(ClO_4)_2$ measured at 1 (1), 50 (2), and 350 (3) μs. The concentration of ***2*** is 2.5×10^{-5} mol/L, the concentration of $Ba(ClO_4)_2$ is 1×10^{-4} mol/L.

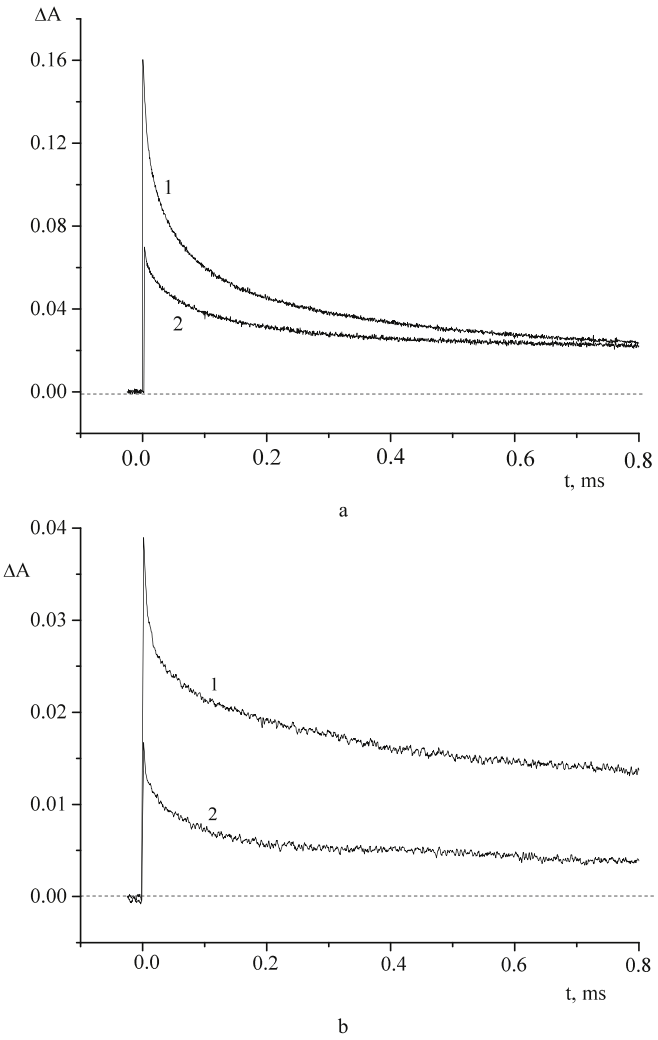

Fig. 9. Kinetic curves of photoinduced absorption of oxygen-free solutions of ***2*** in the presence of $Ba(ClO_4)_2$. The concentrations of $Ba(ClO_4)_2$ is 2×10^{-5} (1) and 5×10^{-4} (2) mol/L. λ = 480 nm (a) and 680 nm (b).

Table 3
Kinetics of photoreaction intermediates in the oxygen-free solutions of ***2*** measured at 480 and 700 nm and different $Ba(ClO_4)_2$ concentrations.

λ, nm	Concentration, mol/L	k_1, s^{-1}	k_2, s^{-1}
480	2×10^{-5}	3.8×10^4	3.6×10^3
	5×10^{-4}	2.3×10^4	3.7×10^3
680	2×10^{-5}	7.0×10^4	2.5×10^3
	5×10^{-4}	2.2×10^4	1.7×10^3

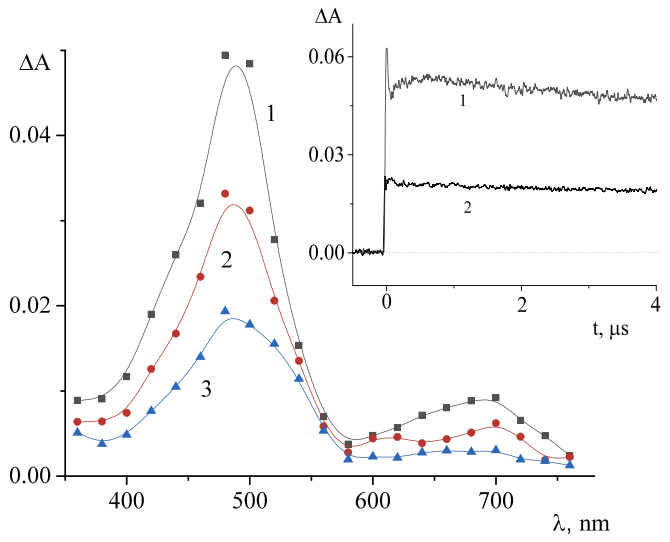

Fig. 10. Photoinduced absorption spectra of the oxygen-free solution of ***2*** in the presence of $Pb(ClO_4)_2$ measured at 1 (*1*), 50 (*2*), and 350 (*3*) μs. The insets shows the kinetic curves of photoinduced absorption of the oxygen-free solutions at 480 nm without (*1*) and with (*2*) $Pb(ClO_4)_2$. The concentration of ***2*** is 2.5×10^{-5} mol/L; the concentration of $Pb(ClO_4)_2$ is 2×10^{-4} mol/L.

electron acceptors on the kinetics of ***2*** was found. The lack of effect on the kinetics can be explained by the fact that the absorption spectra of the radical species overlap with the T-T absorption spectra.

Fig. 8 shows the difference spectrum of photoinduced absorption of ***2*** in the presence of barium perchlorate, and Fig. 9 shows the corresponding kinetic curves.

Table 4
Calculated absorption spectra of the model dye ***2***.

(*E*,*E*)		(*Z*,*E*)		(*Z*,*Z*) rotamer 1		(*Z*,*Z*) rotamer 2	
$S_0 \rightarrow S_n$							
λ, nm	*f*	λ, nm	*f*	λ, nm	*f*	λ, nm	*f*
356	0.80	345	0.72	337	0.56	338	0.11
348	0.13	342	0.11	336	0.02	337	0.40
327	1.34	321	1.00	314	0.71	317	0.57
295	0.04	293	0.05	291	0.07	291	0.14
$S_0 \rightarrow T_n$							
λ, nm		λ, nm		λ, nm		λ, nm	
544		523		486		490	
490		463		456		457	
371		364		359		360	
348		340		334		335	

The difference spectrum of photoinduced absorption is virtually the same as the spectrum measured for the free dye. The kinetic curves are measured at the maxima of photoinduced absorption at 680 nm (a) and 480 nm (b) at different barium perchlorate concentrations.

Table 3 shows the observed rate constants for the decay of induced absorption, which is biexponential, similarly to that of the free dye. The dependence of the rate constants on the metal concentration indicates that the complex composition changes. One can expect that 1:1 complex becomes 1:2 (***2***:Ba^{2+}) as metal concentration increases. Previously, spectrophotometric and fluorescence titration and quantum chemical calculations of ***1*** demonstrated [16] that bis-18-crown-6-di styrylbenzene, unlike bis-15-crown-5-distyrylbenzene, cannot form 2:2 ″double-decker” complexes with barium cation due to the large size of the crown ether cavity.

Fig. 10 shows the difference spectrum and kinetic curves of photoinduced absorption of ***2*** measured in the presence of lead perchlorate.

The kinetic curves of photoinduced absorption measured in the presence of $Pb(ClO_4)_2$ in the maxima of the difference spectrum are almost the same as similar curves measured in the presence of $Ba(ClO_4)_2$. The peculiarity of Pb^{2+} is in that the complexation with $Pb(ClO_4)_2$ is accompanied by the higher probability of the intersystem crossing in ***2*** and decrease in its lifetime due to the heavy atom effect, similarly to ***1*** [17]. This follows from the drastic decrease in the fluorescence quantum yield in the presence of $Pb(ClO_4)_2$ (Table 1). The inset of Fig. 10 illustrates the effect of Pb^{2+} on the phototransformation kinetics of the short-lived photoreaction products. The presence of $Pb(ClO_4)_2$ reduces

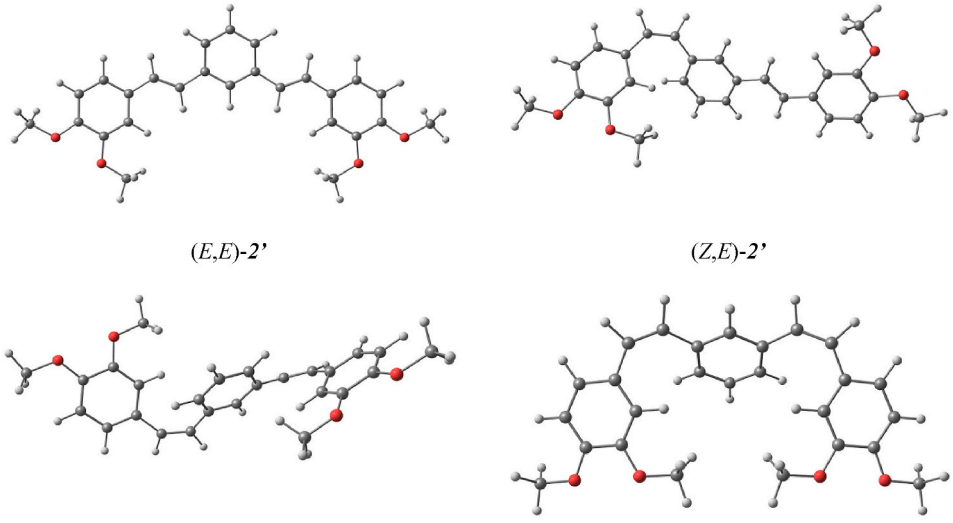

(*E*,*E*)-***2'*** (*Z*,*E*)-***2'***

(*Z*,*Z*)-***2'***, rotamer 1 (*Z*,*Z*)-***2'***, rotamer 2

Fig. 11. The most stable rotamers of *E*- and *Z*-forms of the model dye ***2'***.

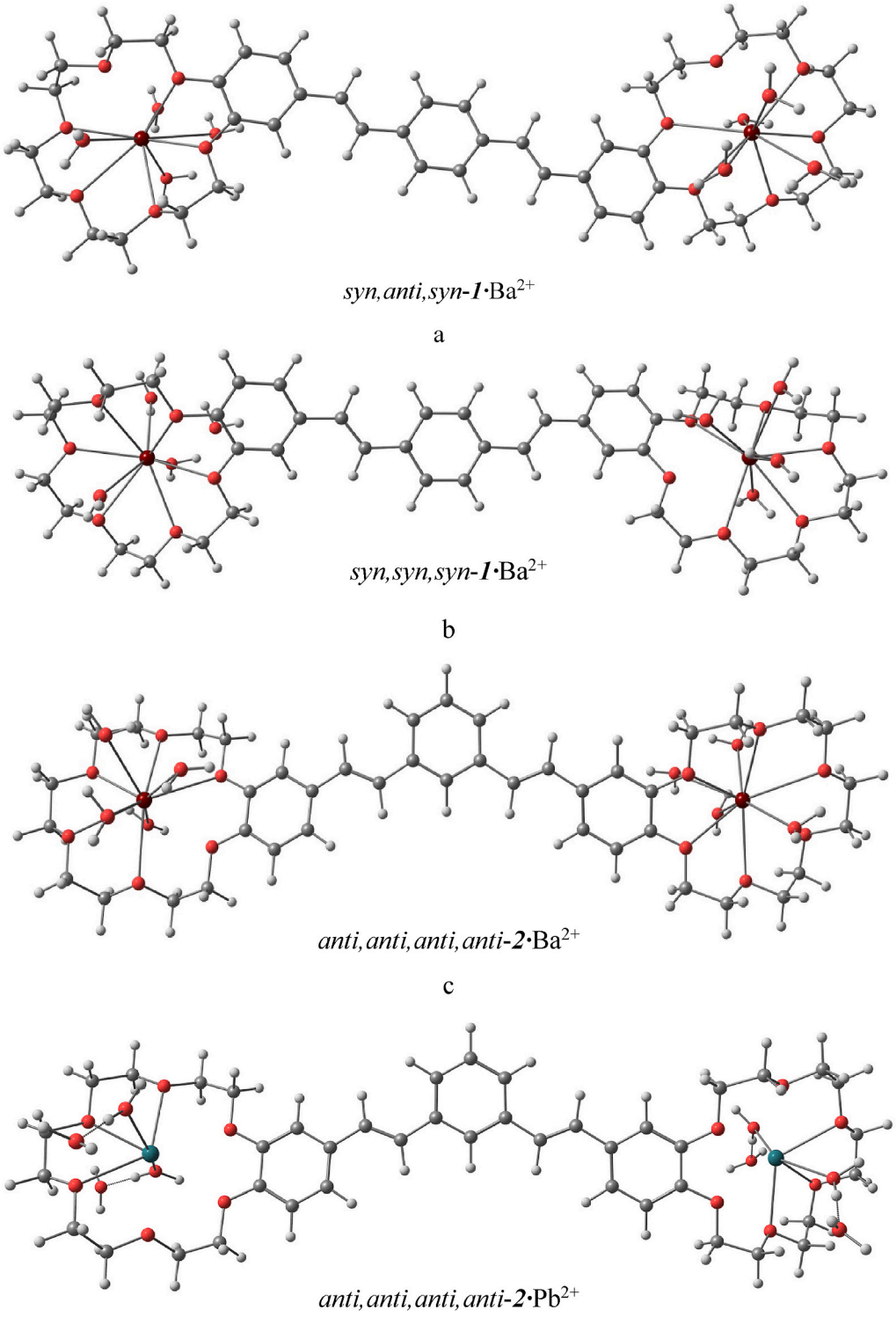

Fig. 12. The most stable rotamers of 2:1 metal complexes with dyes ***1*** (a,b) and ***2*** (c,d).

the dismutation rate and decreases the yield of the radicals. Lack of noticeable changes in the difference spectra measured without (Fig. 4) and with $Pb(ClO_4)_2$ (Fig. 10) can indicate a short triplet lifetime.

4.3. Quantum chemical calculations

Effect of *E-Z*-isomerization on the absorption spectra of the chromophore. The effect of *E-Z*-isomerization on the absorption spectra of the chromophore was theoretically studied for the model dye **2'** containing no crown ether moieties. Its most stable rotamers are shown in Fig. 11.

The calculated spectra (Table 4) show that *E-Z* isomerization leads to a blue shift of the long-wave absorption band. The same effect is observed for the triplet state. This is due to the loss of conjugation in the *Z* form of the chromophore. The experimental data, however, show no photoinduced blue shift, which indicates the lack of *E-Z* isomerization in this system.

Absorption spectra of dye 1 and its complexes with Ba2+. According

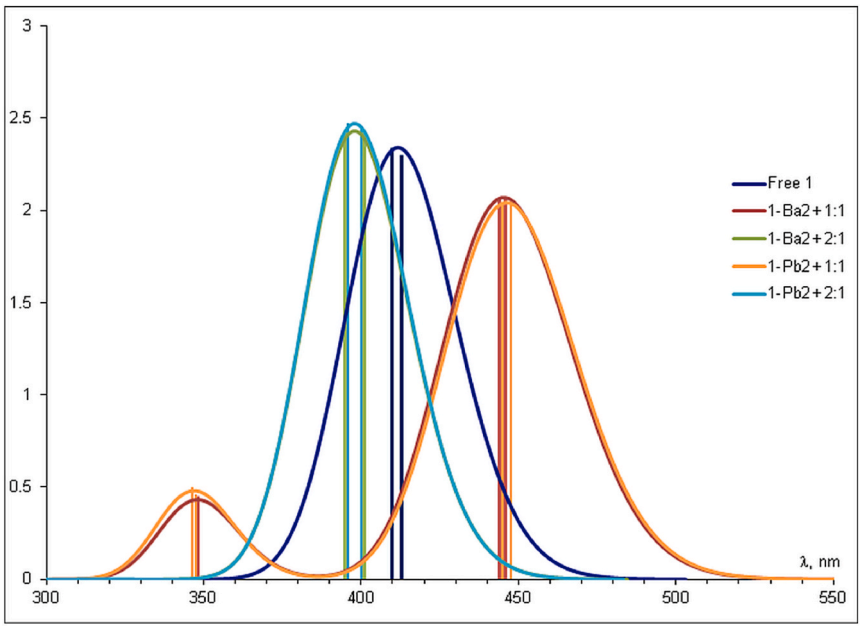

a

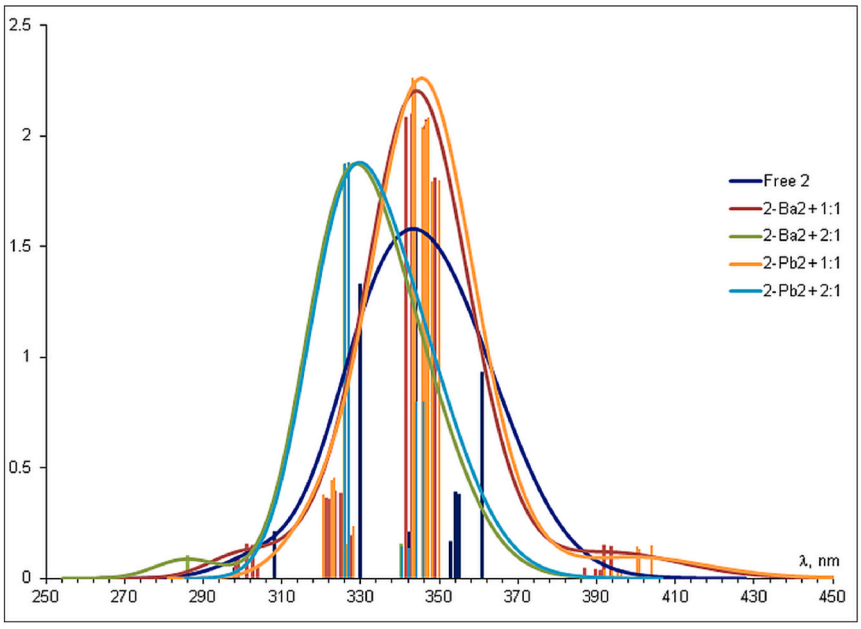

b

Fig. 13. Calculated long wave absorption band of dye ***1*** (a) and ***2*** (b) and their complexes with Ba^{2+} and Pb^{2+} built using Gaussian broadening (0.3 eV) of vertical absorption transitions. Vertical lines show individual vertical transitions.

to Ref. [16], the most stable rotamers of dye ***1*** are *syn,anti,syn*- and *syn, syn,syn*-forms. The structures of their aquacomplexes with Ba^{2+} are shown in Fig. 12 (a).

The calculated spectra of dye ***1*** and its 1:1 and 2:1 complexes with Ba^{2+} are shown in Table S1 of Supporting Information and Fig. 13 (a). Due to strong conjugation, the frontier orbitals (H is for HOMO and L is for LUMO) are delocalized over the entire chromophore.

The 2:1 complex shows a ~12–15 nm blue shift as compared to the free dye, while the 1:1 complex exhibits a ~33–34 nm red shift, because its most intensive transition is of charge transfer character. The computational results agree with the experimental data.

Absorption spectra of dye 2 and its complexes with Ba2+. According to Ref. [21], the most stable rotamers of dye ***2*** are *syn,syn,anti,syn*- and *syn,anti, anti,syn*-forms. However, the complexes show different behavior with respect to the stability of rotamers. In particular, the most stable rotamers of 2:1 complexes are *anti, anti,anti,anti*-forms, while all the rotamers occur with similar frequency in 1:1 complexes. The structures of their aquacomplexes with Ba^{2+} and Pb^{2+} are shown in Fig. 12 (b). Our calculations show that the solvation character and chromophore conformation only slightly affect the stability and spectral properties of the complexes.

The calculated spectra of dye ***2*** and its 1:1 and 2:1 complexes with Ba^{2+} and Pb^{2+} are shown in Fig. 13 (b). In the free dye and its 2:1 complex the frontier orbitals are delocalized over the entire chromophore, while in the 1:1 complex the orbitals are localized on either free part of the chromophore or that complexed with the cation (see

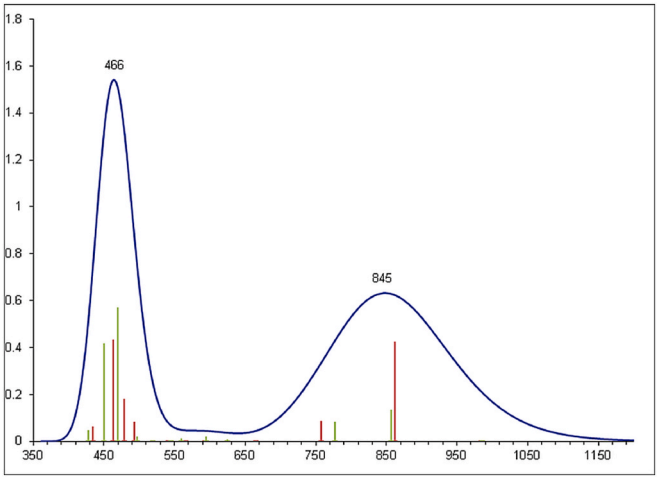

Fig. 14. Calculated T-T absorption spectra of dye ***2*** built using Gaussian broadening (0.3 eV) of vertical absorption transitions. Vertical lines show individual vertical transitions of the two stable rotamers of ***2***.

Supporting Information).

The 2:1 complex shows a ~20-nm blue shift of the absorption band as compared to the free dye. The first (HOMO- > LUMO) transition in the 1:1 complex is red shifted relative to the band of the free dye; however, owing to its low intensity, it does not contribute to the overall absorption of the complex. The main contribution comes from the second transition (HOMO- > LUMO+1) localized on the part of the dye not bonded to the cation, which ensures a negligible shift of the total absorption band of the complex as compared to the free dye. The calculated absorption spectra of Ba^{2+} and Pb^{2+} complexes are very similar. The computational results agree with the experiment.

Triplet states and possible photoproducts of dye *2*. Our calculations show that the energies of two molecules of ***2*** in the relaxed T1 state are higher than the sum energies of $R^{-}\bullet$ and $R^{+}\bullet$ species in the same geometry. This indicates that dismutation process is at least thermodynamically possible.

The calculated T-T absorption spectrum of ***2*** is shown in Fig. 14. The spectrum agrees with the experimental one, which supports the assumption that at least the observed spectra in Fig. 4 are partly due to the T-T absorption.

5. Conclusions

The involvement of the triplet state in the photoreactions of bis(18-crown-6)-1,3-distyrylbenzene ***2*** is established. In addition to T-T absorption, T-T interaction resulting in the $R^{-}\bullet + R^{+}\bullet$ products is suggested to explain the observed microsecond kinetics. In the presence of ascorbic acid as an electron donor, the electron transfer to the radical cation of ***2*** reduces the lifetime of the photoproducts. Pb^{2+} cation reduces the T-T dismutation rate of the triplet molecules and, therefore, the yield of the radicals. Quantum chemical calculations support the assumption that no *E-Z*-isomerization takes place under studied conditions. The calculations also show that the absorption spectra of the 1:1 complexes with Ba^{2+} and Pb^{2+} originate mainly from the absorption of the chromophore portion which is not bound to the cation, while complete complexation (1:2) leads to the blue shift of the long-wave absorption band. Owing to poor conjugation in dye ***2***, the parts of the chromophore are more autonomous as compared to bis(18-crown-6)-1,4-distyrylbenzene ***1***. This manifests itself both as a blue shifted absorption and in the effect of complete and incomplete complexation on the position of the absorption bands. The calculations also support the assumption that the photoinduced absorption spectra originate at least in part from the T-T absorption. At the same time, the possibility of T-T dismutation into $R^{-}\bullet$ and $R^{+}\bullet$ is also demonstrated. The results of this work can be used for the targeted design of photoactive supramolecular assemblies and for the development of optical molecular sensors based on distyrylbenzenes.

Author statement

S.P. Gromov: Conception and design of study, revising the manuscript critically for important intellectual content, **L.S. Atabekyan:** Conception and design of study, acquisition of data, analysis and/or interpretation of data, Drafting the manuscript, Approval of the version of the manuscript to be published, **A.K. Chibisov:** Conception and design of study, revising the manuscript critically for important intellectual content, Approval of the version of the manuscript to be published, **A.Ya. Freidzon:** acquisition of data, analysis and/or interpretation of data, Drafting the manuscript, Approval of the version of the manuscript to be published, **S.Z. Vatsadze:** acquisition of data, Approval of the version of the manuscript to be published, **V.N. Nuriev:** acquisition of data, Approval of the version of the manuscript to be published, **A.V. Medvedko:** Acquisition of data, Approval of the version of the manuscript to be published.

Declaration of competing interest

The authors declare that they have no known competing financial interests or personal relationships that could have appeared to influence the work reported in this paper.

Acknowledgements

Synthesis and steady-state spectroscopy of distyrylbenzene and its complexes was financially supported by the Russian Science Foundation (Project No. 19-13-00020). Laser pulse photolysis and quantum chemical calculations were financially supported by the Ministry of Science and Higher Education of the Russian Federation within the Framework of the State Assignment to the Federal Research Center “Crystallography and Photonics”, Russian Academy of Sciences.

Appendix A. Supplementary data

Supplementary data to this article can be found online at https://doi.org/10.1016/j.dyepig.2020.108773.

References

[1] Alfimov MV, Fedorova OA, Gromov SP. J Photochem Photobiol A 2003;158:183.
[2] Ushakov EN, Gromov SP, Buevich AV, Baskin II, Fedorova OA, Vedernikov AI, et al. J. Chem. Soc., Perkin Trans. 1999;2:601. 3.
[3] Gromov SP, Vedernikov AI, Lobova NA, Kuz'mina LG, Dmitrieva SN, Strelenko YuA, et al. J Org Chem 2014;79:11416.
[4] Ushakov EN, Vedernikov AI, Lobova NA, Dmitrieva SN, Kuz'mina LG, Moiseeva AA, et al. J Phys Chem 2015;119:13025.
[5] Sandros K, Sundahl M, Wennerstrum O, Norinder U. J Am Chem Soc 1990;112:3082.
[6] Marri E, Elisei F, Mazzucato U, Pannacci D, Spalletti A. J Photochem Photobiol A 2006;177:307.
[7] Oelkrug D, Tompert A, Egelhaaf HJ, Hanack M, Steinhuber E, Hohloch M, et al. Synth Met 1996;83:231.
[8] Laughlin BJ, Duniho TL, El Homsi SJ, Levy BE, Deligonul N, Gaffen JR, et al. Org Biomol Chem 2013;11:5425.
[9] Kim M, Whang DR, Gierschnerb J, Park SY. J Mater Chem C 2015;3:231.
[10] Cavazzini M, Quici S, Orlandi S, Sissa C, Terenziani F, Painelli A. Tetrahedron 2013;69:2827.
[11] Chaieb A, Khoukh A, Brown R, Francois J, Dagron-Lartigau C. Opt Mater 2007;30:318.
[12] Kalanoor BS, Bisht PB, Annamalai S, Aidhen IS. J Lumin 2009;129:1094.
[13] Motoyoshiya J, Fengqiang Z, Nishii Y, Aoyama H. Spectrochim Acta A 2008;69:167.
[14] Pond SJK, Tsutsumi O, Rumi M, Kwon O, Zojer E, Bredas JL, et al. J Am Chem Soc 2004;126:9291.
[15] Vatsadze SZ, Gromov SP. Macroheterocycles 2017;10:432.
[16] Vedernikov AI, Nuriev VN, Fedorov OV, Moiseeva AA, Kurchavov NA, Kuz'mina LG, et al. Russ Chem Bull 2016;65:2686.
[17] Atabekyan LS, Avakyan VG, Chibisov AK, Gromov SP, Vatsadze SZ, Nuriev VN, et al. High Energy Chem 2019;53:115.

[18] Mochida S, Hirano K, Satoh T, Miura M. J Org Chem 2011;76:3024.
[19] Toyoshima T, Yoshida S, Watanabe S. Tetrahedron 2013;69:1904.
[20] Meier H. Angew Chem, Int Ed Engl 1992;31:1399.
[21] Zertani R, Meier H. Chem Ber 1986;119:1704.
[22] Yang Shi-Yao, Naumov P, Fukuzumi S. J Am Chem Soc 2009;131:7247.
[23] Marri E, Galiazzo G, Mazzucato U, Spalletti A. Chem Phys 2005;312:205.
[24] Nuriev VN, Fedorov OV, Moiseeva AA, Freidzon AYa, Kurchavov NA, Vedernikov AI, et al. Russ J Org Chem 2017;53:1689.
[25] Vedernikov AI, Basok SS, Gromov SP, Kuz'mina LG, Avakyan VG, Lobova NA, et al. Russ J Org Chem 2005;41:843.
[26] Gromov SP, Vedernikov AI, Lobova NA, Kuz'mina LG, Basok SS, Strelenko YA, et al. New J Chem 2011;35:724.
[27] Atabekyan LS, Aleksandrova NA, Vedernikov AI, Lobova NA, Gromov SP, Chibisov AK. High Energy Chem 2017;51:189.
[28] Atabekyan LS, Lobova NA, Vedernikov AN, Gromov SP, Chibisov AK. High Energy Chem 2012;46:100.
[29] Perry JW, Mansour K, Marder SR, Perry KJ, Alvarez D, Choong I. Optic Lett 1994; 19:625.
[30] Atabekyan LS, Chibisov AK, Alfimov MV. High Energy Chem 1997;31:344.
[31] Montalti M, Kpedi A, Prodi L, Gandolfi MT. Handbook of phochemistry. third ed. London: Taylor and Fransis; 2006. p. 574.
[32] Laikov DN. Chem Phys Lett 1997;28:151.
[33] Laikov DN, Ustynyuk YA. Russ Chem Bull 2005;54:820.
[34] Kaupp M, Schleyer PvR, Stoll H, Preuss H. J Chem Phys 1991;94:1360.
[35] Stevens WJ, Krauss M, Basch H, Jasien PG. Can J Chem 1992;70:612.
[36] Weigend F, Ahlrichs R. Phys Chem Chem Phys 2005;7:3297.
[37] Cossi M, Rega N, Scalmani G, Barone V. J Chem Phys 2001;114:5691.
[38] Granovsky AA. Firefly, version 8.2.0. 2017. http://classic.chem.msu.su/gran/firefly/index.html.
[39] Schmidt MW, Baldridge KK, Boatz JA, Elbert ST, Gordon MS, Jensen JJ, et al. J Comput Chem 1993;14:1347.
[40] Freidzon AYa, Bagatur'yants AA, Gromov SP, Alfimov MV. Russ Chem Bull (Int Ed) 2008;57:2009.
[41] Lednev IK, Hester RE, Moore JN. J Chem Soc, Faraday Trans 1997;93:1551. 2.
[42] Freidzon AYa, Bagatur'yants AA, Gromov SP, Alfimov MV. RussChem Bull, (Int Ed) 2005;54:2042.
[43] Freidzon AYa, Vladimirova KG, Bagatur'yants AA, Gromov SP, Alfimov MV. J Mol Struct: Theochem. 2007;809:61.
[44] Freidzon AYa, Bagatur'yants AA, Gromov SP, Alfimov MV. Int J Quant Chem 2004; 100:617.
[45] Freidzon AY, Bagatur'yants AA, Ushakov EN, Gromov SP, Alfimov MV. Int J Quant Chem 2011;111:2649.
[46] Korobov VE, Chibisov AK. Usp Khim 1983;52(1):43.